

SlyD Proteins from Different Species Exhibit High Prolyl Isomerase and Chaperone Activities[†]

Christian Scholz,^{*,‡} Barbara Eckert,[§] Franz Hagn,^{§,||} Peter Schaarschmidt,[‡] Jochen Balbach,^{§,⊥} and Franz Xaver Schmid[§]

Roche Diagnostics GmbH, Nonnenwald 2, D-82377 Penzberg, Germany, and Laboratorium für Biochemie, Universität Bayreuth, D-95440 Bayreuth, Germany

Received September 21, 2005; Revised Manuscript Received November 7, 2005

ABSTRACT: SlyD is a putative folding helper protein from the *Escherichia coli* cytosol, which consists of an N-terminal prolyl isomerase domain of the FKBP type and a presumably unstructured C-terminal tail. We produced truncated versions without this tail (SlyD*) for SlyD from *E. coli*, as well as for the SlyD orthologues from *Yersinia pestis*, *Treponema pallidum*, *Pasteurella multocida*, and *Vibrio cholerae*. They are monomeric in solution and unfold reversibly. All SlyD variants catalyze the proline-limited refolding of ribonuclease T1 with very high efficiencies, and the specificity constants (k_{cat}/K_M) are equal to $\sim 10^6 \text{ M}^{-1} \text{ s}^{-1}$. These large values originate from the high affinities of the SlyD orthologues for unfolded RCM-T1, which are reflected in low K_M values of $\sim 1 \mu\text{M}$. SlyD also exhibits pronounced chaperone properties. Permanently unfolded proteins bind with high affinity to SlyD and thus inhibit its prolyl isomerase activity. The unfolded protein chains do not need to contain proline residues to be recognized and bound by SlyD. The conservation of prolyl isomerase activity and chaperone properties within the SlyD family suggests that these proteins might act as true folding helpers in the bacterial cytosol. The SlyD proteins are also well suited for biotechnological applications. As fusion partners they facilitate the refolding and increase the solubility of aggregation-prone proteins such as the gp41 ectodomain fragment of HIV-1.

Protein folding is a spontaneous process that is driven by the small difference in Gibbs free energy between the native and unfolded state (1–3). Aggregation of incompletely folded molecules competes with productive folding, and this constitutes a major problem both in vitro and in vivo (4, 5). In living cells, folding is assisted by helper proteins (6–8). Folding catalysts such as disulfide oxidoreductases and peptidyl-prolyl *cis/trans*-isomerases accelerate slow steps in protein folding and thus shorten the lifetime of folding intermediates, whereas chaperones bind to unfolded or partially folded protein segments and thus prevent aggregation (9–14). Ideal folding helpers should combine chaperone and enzyme properties, and in fact, several disulfide isomerases and prolyl isomerases are also chaperones. These folding helpers with dual or multiple functions should also be valuable for the production of recombinant proteins.

In the periplasm of *Escherichia coli* (15), the oxidoreductases DsbA and DsbC introduce and isomerize disulfide

bonds in folding proteins (16–20). FkpA¹ and SurA mediate the folding of translocated protein chains and combine both prolyl isomerase and chaperone function (21–24). In the cytoplasm, the trigger factor and SlyD also possess prolyl isomerase activity and chaperone properties. There is good evidence now that the trigger factor is a chaperone for nascent protein chains at the ribosome (25–27). Little is known about the physiological role of SlyD. Earlier speculation that SlyD might be involved in the hydrogenase biosynthetic pathway of *E. coli*, probably by aiding the assembly of [Ni-Fe] clusters as a metallochaperone (28, 29), has recently been corroborated (30).

¹ Abbreviations: FkpA, FK506 binding protein A, periplasmic *E. coli* chaperone; SlyD, sensitive to lysis D, cytosolic *E. coli* chaperone; RNase T1, ribonuclease T1; RCM-T1, disulfide-reduced and S-carboxymethylated form of a variant of RNase T1 with Ser54 and Pro55 replaced with Gly and Asn, respectively; RCM-T1-P39A, disulfide-reduced and S-carboxymethylated form of a variant of RNase T1 with Pro39 replaced with Ala; RCM- α -La, disulfide-reduced and S-carboxymethylated form of bovine α -lactalbumin; RCM-Ten-P7A/P9A/P50A, disulfide-reduced and S-carboxymethylated form of the proline-free (P7A/P9A/P50A) mutant of the α -amylase inhibitor Tendamistat; PPIase, peptidyl-prolyl *cis/trans* isomerase; GdmCl, guanidinium chloride; Ni-NTA, nickel nitrilotriacetate; SDS, sodium dodecyl sulfate; PAGE, polyacrylamide gel electrophoresis; FPLC, fast protein liquid chromatography; TCEP, tris(2-carboxyethyl)phosphine; Tricine, N-tris(hydroxymethyl)methylglycine; CD, circular dichroism; HIV-1, human immunodeficiency virus type 1; gp41, transmembrane glycoprotein with 41 kDa from HIV-1; hFKBP12, human FK506 binding protein with 12 kDa; TcFKBP18, FK506 binding protein with 18 kDa from *Thermococcus* sp. KS-1; MtFKBP17, FK506 binding protein with 17 kDa from *Methanococcus thermolithotrophicus*. Elecsys and Complete are trademarks of Roche.

[†] This research was supported by the Deutsche Forschungsgemeinschaft (BA1821/2-1, GRK1026/1, and Schm444/17-1) and by INTAS-2001-2347.

* To whom correspondence should be addressed: Roche Diagnostics GmbH, Department LR-IR, Nonnenwald 2, D-82377 Penzberg, Germany. Phone: ++49-8856-603878. Fax: ++49-8856-605265. E-mail: christian.scholz@roche.com.

[‡] Roche Diagnostics GmbH.

[§] Universität Bayreuth.

^{||} Present address: Lehrstuhl für Organische Chemie II, TU München, D-85747 Garching, Germany.

[⊥] Present address: Fachbereich Physik, Fachgruppe Biophysik, Universität Halle-Wittenberg, D-06099 Halle, Germany.

SlyD was originally discovered as a persistent contaminant of recombinant proteins that had been purified by immobilized metal affinity chromatography (IMAC) (29, 31, 32). The N-terminal part of SlyD encompasses a FKBP-like prolyl isomerase domain with a weak affinity for proline-containing short peptides (29). The k_{cat}/K_M values for the catalysis of prolyl isomerization in peptides are low and range between 6000 and 29 000 $\text{M}^{-1} \text{s}^{-1}$ (28, 33). Since SlyD is very susceptible to proteolysis, its prolyl isomerase activity is barely detectable in the chymotrypsin-coupled standard assay (28, 29, 33, 34). The C-terminal part of SlyD is rich in cysteine and histidine residues and therefore binds tightly to divalent cations such as Ni^{2+} , Zn^{2+} , Cu^{2+} , and Co^{2+} (29). The binding of Ni^{2+} in the C-terminal region reversibly inhibits the prolyl isomerase activity of SlyD (28).

SlyD plays a pivotal role as a host factor for the ϕX174 lysis cycle by stabilizing the hydrophobic viral lysis protein E, possibly by a chaperone-like mechanism (35–37). *E. coli* variants with mutations in the *slyD* gene are resistant to lysis by the bacteriophage ϕX174 ; hence, its actual designation is sensitivity to lysis D (38).

The isolated N-domain of SlyD is active as a prolyl isomerase (28) and possibly harbors both prolyl isomerase and chaperone activity. Such a combination would increase the affinity for incompletely folded protein chains and thus increase the overall folding activity in a manner found previously for the trigger factor (27, 39–41), SurA (22, 42), and DsbA (43). Trigger factor forms complexes with unfolded proteins that show K_D values in the 0.1–1 μM range (41, 44, 45) and are highly dynamic (46). This renders trigger factor one of the most efficient prolyl isomerases known to date (40, 41, 47).

Here we examine the catalytic efficiency of SlyD as a catalyst of the refolding of the reduced and carboxymethylated form of ribonuclease T1 (RCM-T1). This refolding reaction is limited in rate by a prolyl *trans*–*cis* isomerization and thus well suited for investigation of the catalytic properties of prolyl isomerases (48–50). We asked whether the chaperone function and the enzymatic activity of SlyD both reside in the N-terminal FKBP-like domain [residues 1–146 (28, 29)]. Truncated forms of SlyD that varied in length and contained different parts of the cysteine- and histidine-rich C-terminal tail (SlyD 1–196, wt-SlyD; SlyD 1–165, SlyD*; SlyD 1–148, SlyD**) were characterized. In addition, we addressed the question of whether the prolyl isomerase and chaperone properties are conserved in SlyD homologues from different species. To this end, we characterized the SlyDs from *E. coli*, *Vibrio cholerae*, *Pasteurella multocida*, *Treponema pallidum*, and *Yersinia pestis*.

Recently, we found that the covalent fusion with the *E. coli* chaperones SlyD and FkpA enhanced the cytosolic expression and the solubility of aggregation-prone proteins. Notably, SlyD and FkpA exerted their beneficial solubilizing effect during *in vitro* refolding and thus paved the way for the convenient and high-yield renaturation of extremely aggregation-prone proteins into a soluble and functional conformation (51). Here we ask whether this high solubilization potential is conserved in the SlyD proteins from different bacteria.

MATERIALS AND METHODS

Materials and Reagents. GdmCl (A-grade) was purchased from NIGU (Waldkraiburg, Germany). Complete EDTA-free protease inhibitor tablets, L-lysine, imidazole, and EDTA were from Roche Diagnostics GmbH (Mannheim, Germany), and all other chemicals were analytical grade and from Merck (Darmstadt, Germany). Citrate synthase was purchased from Roche Diagnostics GmbH, and α -lactalbumin was from Sigma (St. Louis, MO). (S54G,P55N)-RNase T1 was purified as described previously (52). The permanently unfolded proteins for SlyD* inhibition (RCM- α -La, RCM-Ten-P7A/P9A/P50A, and RCM-T1-P39A) were prepared by reduction and carboxymethylation as described for wild-type RNase T1 (52). FK506 was a kind gift of Fujisawa Pharmaceutical Corp. Ltd. (Osaka, Japan). Ultrafiltration membranes (YM10 and YM30) were purchased from Amicon (Danvers, MA), and microdialysis membranes (VS/0.025 μm) and ultrafiltration units (biomax ultrafree filter devices) were from Millipore (Bedford, MA). Cellulose nitrate and cellulose acetate membranes (1.2, 0.45, and 0.2 μm) for the filtration of crude lysates were from Sartorius (Göttingen, Germany).

Cloning of Expression Cassettes. The sequences of the SlyD orthologues from *E. coli* (accession number P0A9K9), from *Y. pestis* (accession number Q8ZJC2), from *P. multocida* (accession number Q9CKP2), from *V. cholerae* (accession number Q9KNX6), and from *T. pallidum* (accession number O83369) were retrieved from the SwissProt database. Synthetic genes encoding the various SlyD orthologues and human FKBP12 were purchased from Medigenomix (Martinsried, Germany) and cloned into pET24 expression vectors (Novagen, Madison, WI). The codon usage was optimized for expression in *E. coli* host cells. The expression cassettes for the various fusion proteins were designed as described for the *E. coli* SlyD* fusion module (51). QuikChange (Stratagene, La Jolla, CA) and standard PCR techniques were used to generate point mutations, deletion variants, or restriction sites. Except wild-type SlyD from *E. coli*, all recombinant SlyD variants as well as hFKBP12 contained a C-terminal hexahistidine tag to facilitate Ni-NTA-assisted purification (53) and refolding.

Expression, Purification, and Refolding of SlyD Variants and Fusion Proteins. All SlyD variants and human FKBP12 were purified by using virtually identical protocols. *E. coli* BL21(DE3) cells harboring the particular pET24a expression plasmid were grown at 37 °C in LB medium with kanamycin (30 $\mu\text{g}/\text{mL}$) to an OD_{600} of 1.5, and cytosolic overexpression was induced by adding 1 mM isopropyl β -D-thiogalactoside. Three hours after induction, cells were harvested by centrifugation (20 min at 5000g), frozen, and stored at –20 °C. For cell lysis, the frozen pellet was resuspended in chilled 100 mM sodium phosphate (pH 8.0), 7.0 M GdmCl, and 10 mM imidazole, and the suspension was stirred for 2 h on ice to complete cell lysis. After centrifugation and filtration (cellulose nitrate membrane, 0.45 and 0.2 μm), the lysate was applied onto a Ni-NTA column equilibrated with the lysis buffer, including 2.5 mM TCEP. The subsequent washing step was tailored for the respective target protein and ranged from 5 to 15 mM imidazole for the SlyD variants and from 10 to 25 mM imidazole [in 50 mM sodium phosphate (pH 8.0), 7.0 M GdmCl, and 2.5 mM TCEP] for the SlyD fusion proteins. At least 10–15 volumes of the

Table 1: Spectroscopic and Stability Parameters of SlyD Variants^a

	extinction coefficient ϵ_{280} ($M^{-1} \text{ cm}^{-1}$)	$\Delta\epsilon_{288}$ ($M^{-1} \text{ cm}^{-1}$)	melting temperature ($^{\circ}\text{C}$)	
			absorbance at 288 nm	CD at 278 nm
<i>E. coli</i> SlyD(1–196) wild type	5950	1196	41.5	42.8
<i>E. coli</i> SlyD*(1–165)	5788	1530	41.5	43.5
<i>E. coli</i> SlyD*(1–148)	5654	1390	nd ^b	nd ^b
<i>Y. pestis</i> SlyD(1–165)	5500	1257	31.2	33.4
<i>V. cholerae</i> SlyD(1–157)	4550	1608	41.9	41.8
<i>T. pallidum</i> SlyD(1–160)	4356	1183	38.2	39.2
<i>P. multocida</i> SlyD(1–156)	5910	1565	50.4	49.5

^a Extinction coefficients were determined according to the method of Gill and von Hippel (55). CD-detected unfolding transitions were measured at a protein concentration of 250 μM and monitored at 278 nm. UV-detected unfolding transitions were performed at a protein concentration of 100 μM and monitored at 288 nm. Buffer conditions were 50 mM sodium phosphate (pH 7.5), 100 mM NaCl, and 1 mM EDTA. ^b Not determined.

washing buffer were applied. Then, the GdmCl solution was replaced with 50 mM sodium phosphate (pH 7.8), 100 mM NaCl, 5 mM imidazole, and 2.5 mM TCEP to induce conformational refolding of the matrix-bound protein. To avoid reactivation of copurifying proteases, a protease inhibitor cocktail (Complete EDTA-free, Roche) was included in the refolding buffer. A total of 15–20 column volumes of refolding buffer was applied in an overnight reaction. Then, both TCEP and the Complete EDTA-free inhibitor cocktail were removed by washing with 3–5 column volumes of 50 mM sodium phosphate (pH 7.8), 100 mM NaCl, and 5 mM imidazole. The native protein was then eluted with 250 mM imidazole in the same buffer. Protein-containing fractions were assessed for purity by Tricine–SDS–PAGE (54) and pooled. Finally, the proteins were subjected to size-exclusion chromatography (Superdex HiLoad, Amersham Pharmacia), and the protein-containing fractions were pooled and concentrated in an Amicon cell (YM10). Trigger factor from *E. coli* was purified as described previously (46).

Spectroscopic Measurements. Protein concentration measurements were performed with a Uvikon XL double-beam spectrophotometer. The molar extinction coefficients (ϵ_{280}) were determined experimentally by using the procedure described by Gill and von Hippel (55); they are given in Table 1. The ϵ_{280} values for the fusion proteins were calculated according to the method of Pace (56).

Thermally induced unfolding and refolding of SlyD* were followed by the change in absorbance at 288 nm in a Hewlett-Packard diode array photometer. The proteins were diluted to 10 and 100 μM in 50 mM sodium phosphate (pH 7.5), 100 mM NaCl, and 1 mM EDTA. To prevent cysteine oxidation, the thermally induced unfolding transitions of wild-type SlyD were measured in the presence of 2 mM TCEP. Heating and cooling rates were 1 $^{\circ}\text{C}/\text{min}$.

Near-UV CD spectra were recorded with a Jasco-720 spectropolarimeter with a thermostated cell holder and converted to mean residue ellipticity. The buffer was 50 mM sodium phosphate (pH 7.5), 100 mM NaCl, and 1 mM EDTA. The path length was 0.5 or 1.0 cm, and the protein concentration was 20–500 μM . The bandwidth was 1 nm; the scanning speed was 20 nm/min at a resolution of 0.5 nm, and the response was 2 s. To improve the signal-to-noise ratio, spectra were measured nine times and averaged.

For the thermal unfolding transitions of the SlyD variants, the proteins were diluted to concentrations of 25 and 250

μM in 50 mM sodium phosphate (pH 7.5), 100 mM NaCl, and 1 mM EDTA. Thermally induced unfolding–refolding transitions were recorded at 278 nm under gentle stirring, and the path length of the cuvette was 1.0 cm. Heating and cooling rates were 1 $^{\circ}\text{C}/\text{min}$, and the response time was 4 s. To assess the reversibility of unfolding, near-UV CD spectra of the SlyD variants were recorded before and after the thermally induced unfolding–refolding cycle.

Citrate Synthase Aggregation Assay. The assay was performed essentially as outlined by Buchner et al. (57). Citrate synthase was unfolded at 25 $^{\circ}\text{C}$ in 6.0 M GdmCl, 20 mM DTE, and 50 mM Tris-HCl (pH 8.0) for 1 h and then diluted 100-fold to a final concentration of 0.15 μM (monomer) in 60 mM GdmCl, 50 mM NaCl, 0.2 mM DTE, 50 mM Tris-HCl (pH 8.0), and varying SlyD concentrations at 25 $^{\circ}\text{C}$. Spontaneous aggregation was monitored by the increase in light scattering at 360 nm in a Hitachi F4010 fluorescence spectrometer.

Folding Experiments. RCM-T1 was unfolded by incubating the protein in 0.1 M Tris-HCl (pH 8.0) at 15 $^{\circ}\text{C}$ for at least 1 h. Refolding at 15 $^{\circ}\text{C}$ was initiated by a 40-fold dilution of the unfolded protein to final conditions of 2.0 M NaCl and the desired concentrations of SlyD, RCM-T1, and the inhibitory unfolded proteins (if appropriate) in the same buffer. The folding reaction was followed by the increase in protein fluorescence at 320 nm (10 nm bandwidth) after excitation at 268 nm (1.5 nm bandwidth). The unfolded inhibitory proteins (bovine RCM- α -La, RCM-Ten-P7A/P9A/P50A, and RCM-T1-P39A) contain tryptophan residues, and their contributions to the fluorescence were subtracted from the measured values in the individual experiments. At 2.0 M NaCl, slow folding of RCM-T1 was a monoexponential process, and its rate constant was determined by using GraFit 3.0 (Erithacus Software, Staines, U.K.).

Enzyme Kinetics of Catalyzed Folding. To analyze the enzyme kinetics of catalyzed folding and its inhibition by unfolded proteins, we measured the kinetics of folding in the presence of 20 nM SlyD* and (in the inhibition experiments) of various concentrations of unfolded protein chains under the folding conditions described above. Both catalyzed and uncatalyzed folding occur in these experiments. The initial velocities of catalyzed folding were determined from the measured progress curves by using the procedure originally developed for the analysis of enzyme-catalyzed prolyl isomerization in a peptide (58) as adapted for the analysis of the catalyzed folding of RCM-T1 (41, 45). The

time course of folding in the presence of SlyD* is described by the differential equation (eq 1)

$$d[U]/dt = -k_0[U] - k_{\text{cat}}[\text{SlyD}^*][U]/([U] + K_M) \quad (1)$$

where $d[U]/dt$ is the rate of folding of the unfolded protein U , $-k_0[U]$ is the contribution of uncatalyzed folding, and $-k_{\text{cat}}[\text{SlyD}^*][U]/([U] + K_M)$ is the contribution of catalyzed folding. k_{cat} and K_M are the catalytic rate constant and the Michaelis constant, respectively, and $[\text{SlyD}^*]$ is the concentration of SlyD*. A nonlinear least-squares fit of the observed folding kinetics to eq 1 was performed by using Scientist (MicroMath, St. Louis, MO). In the analysis, the fact that only 85% of the unfolded RCM-T1 molecules contain an incorrect *trans* Pro39 (49) was accounted for, i.e., $[U]_0 = 0.85[\text{RCM-T1}]$. The slow refolding reaction, which is analyzed here, originates from these molecules. The rate constant of uncatalyzed folding ($k_0 = 0.00173 \text{ s}^{-1}$) was measured in folding experiments in the absence of SlyD* between 0.1 and 10 μM RCM-T1. This value was used when the experimental data were fitted to eq 1. The values for k_{cat} and K_M as obtained from this analysis were then used to calculate the initial rates of catalyzed folding v_0 at the different substrate concentrations from eq 2. In this equation, the initial value of $[U]_0$ is 0.85[RCM-T1].

$$v_0 = k_{\text{cat}}[\text{SlyD}^*][U]_0/([U]_0 + K_M) \quad (2)$$

The contribution $-k_0[U]$ from uncatalyzed folding (eq 1) increases linearly with the concentration of RCM-T1 and dominates the observed folding kinetics at high RCM-T1 concentrations. Therefore, data at RCM-T1 concentrations higher than 20 μM were not used for the analysis.

Immunological Reactivity of SlyD*–gp41 Fusion Proteins. The different SlyD*–gp41 fusion proteins were used to detect anti-gp41 antibodies, which abundantly occur in HIV-1 positive sera. The immunological reactivity was challenged in an automated Elecsys 2010 analyzer using the double-antigen sandwich format.

Signal detection in the Elecsys immunoassay is based on electrochemoluminescence. The biotin conjugate (i.e., the capture antigen) is immobilized on the surface of a streptavidin-coated magnetic bead, whereas the signaling antigen bears a complexed ruthenium cation as the luminiscent moiety. In the presence of anti-gp41 antibodies, the chromogenic ruthenium complex is bridged to the solid phase and emits light at 620 nm after excitation at a platinum electrode. The signal output is in arbitrary light units. For their use as Elecsys antigens, the soluble gp41 fusion proteins being studied were concentrated and modified with *N*-hydroxysuccinimide-activated biotin and ruthenium moieties as described previously (51). The concentration of the gp41 variants in the immunoassay measurements was $\sim 750 \text{ ng/mL}$. At least five negative sera were used as controls. To minimize false positive results, polymerized unlabeled *E. coli* SlyD* was added to the samples as an anti-interference substance.

RESULTS

Expression and Refolding of SlyD*. SlyD*(1–165) from *E. coli*, SlyD*(1–165) from *Y. pestis*, SlyD*(1–156) from *P. multocida*, SlyD*(1–157) from *V. cholerae*, and SlyD*–

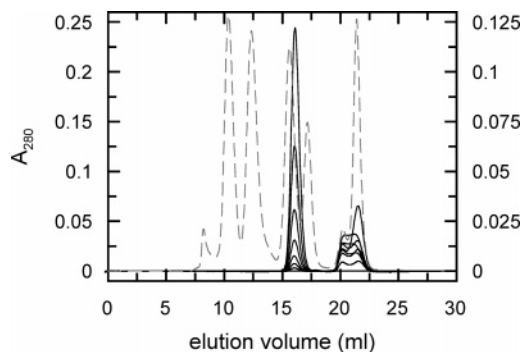


FIGURE 1: Analytical gel filtration of *E. coli* SlyD*(1–165) at varying protein concentrations on a Superdex 200 HR 10/30 gel filtration column. Two hundred microliters of a 180, 90, 45, 22.5, 11.25, 5.6, and 2.8 μM SlyD* solution was applied on the SEC column, and elution was monitored at 280 nm (left ordinate). The Roche FPLC standard (gray dotted line, right ordinate) contains β -galactosidase (465 kDa), sheep IgG (150 kDa), sheep IgG Fab fragment (50 kDa), horse myoglobin (17 kDa), and the dipeptide Gly-Tyr (0.238 kDa). SlyD* elutes invariably at $\sim 16.1 \text{ mL}$, suggestive of an apparent dimer.

(1–160) from *T. pallidum* were produced in large amounts in *E. coli* BL21(DE3) cells. Due to the high rate of synthesis, a fraction of the protein formed insoluble aggregates in the host cytosol. During cell lysis, the proteins were solubilized in 7.0 M GdmCl and, after centrifugation and filtration, bound to a Ni–NTA column. Refolding on the column was initiated by washing with 50 mM sodium phosphate and 5 mM imidazole buffer, and the refolded protein was eluted with 250 mM imidazole. After this coupled purification and refolding, $\sim 30 \text{ mg}$ of SlyD*/g of *E. coli* cells was obtained. The purity of the various SlyD* homologues after the refolding chromatography exceeded 95% as assessed by Tricine–SDS–PAGE (54). Denaturant-unfolded wild-type SlyD from the *E. coli* host has been reported to bind with high affinity to Ni–NTA columns (34, 59). Unfolding of wild-type SlyD in 7.0 M GdmCl (pH 8.0) probably leads to disulfide-linked SlyD oligomers with increased affinity for the metal support. By optimizing the imidazole concentration and including the reducing agent TCEP during the metal ion chromatography, we could prevent contamination of the C-terminally truncated SlyD homologues by the wild-type SlyD from the *E. coli* host.

Full-length SlyD has been described as a dimeric protein (59, 60). The truncated SlyD variant from *E. coli*, SlyD*–(1–165), elutes from a Superdex 200 gel filtration column at a position that is also suggestive of a dimer (Figure 1). However, the position of this elution peak is independent of the protein concentration. Equilibrium ultracentrifugation experiments showed that SlyD* is in fact monomeric in solution (H. Lilie, unpublished results). It is possible that an elongated shape of SlyD* leads to the peculiar elution from the gel filtration column. The SlyD* proteins from *Y. pestis* (1–165), from *P. multocida* (1–156), from *V. cholerae* (1–157), and from *T. pallidum* (1–160) all show the same elution behavior.

It should be noted that the *P. multocida* variant has been deposited in the TrEMBL protein sequence database as an FkpA homologue (accession number Q9CKP2). Its length, its high degree of homology (for alignment, see Figure 2), and its C-terminal tail rich in histidine and cysteine residues, however, rather point to a close relationship with SlyD. To

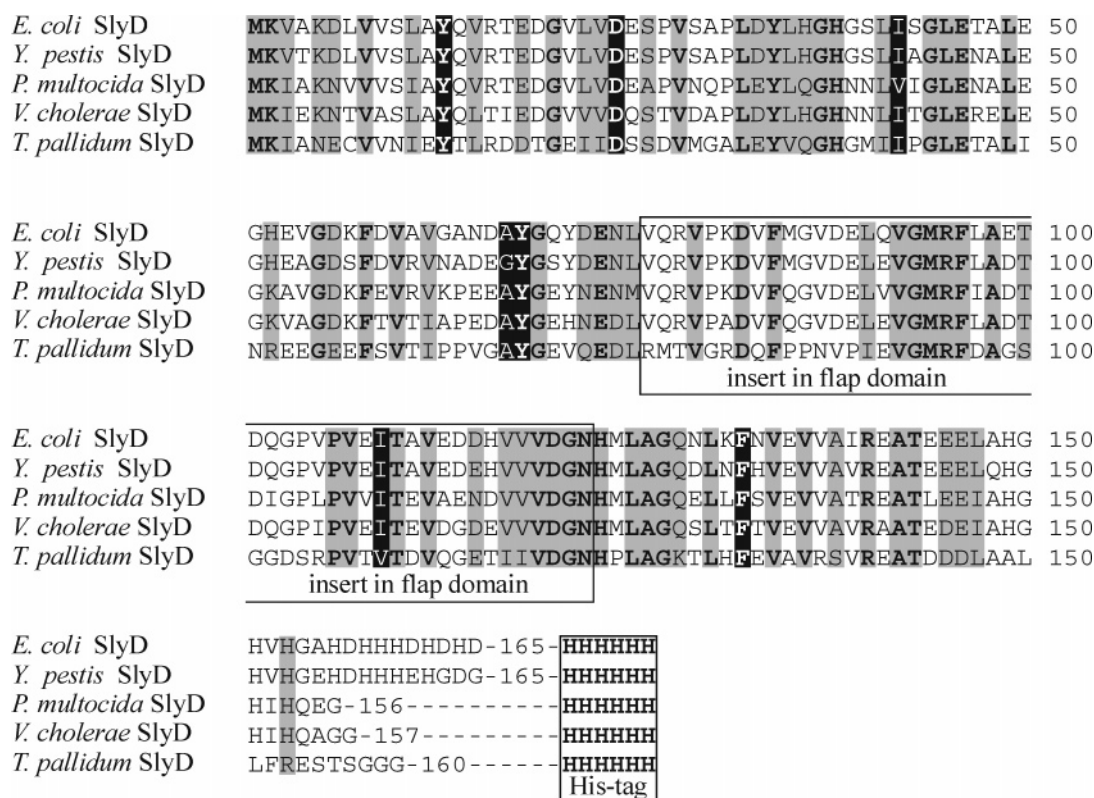


FIGURE 2: Sequence alignment of SlyD* variants lacking the cysteine-rich C-terminal tail, as performed by CLUSTAL W (1.82) (122, 123). Shown are the SlyD orthologues from *E. coli* (1–165, SwissProt accession number P0A9K9), from *Y. pestis* (1–165, SwissProt accession number Q8ZJC2), from *P. multocida* (1–156, SwissProt accession number Q9CKP2), from *V. cholerae* (1–157, SwissProt accession number Q9KNX6), and from *T. pallidum* (1–160, SwissProt accession number O83369). Amino acids assumed to be essential for FK506 binding (28, 73) are printed in white letters on a black background. Identical amino acids are indicated by bold print, and identical and conserved amino acids are highlighted by a gray background. The insert in the flap region (98) is boxed, as well as the C-terminal hexahistidine purification tag.

harmonize nomenclature and to facilitate reading, we therefore denote this enzyme *P. multocida* SlyD.

Truncated SlyD* Variants Unfold Reversibly. Previously, we had found that thermal and GdmCl-induced unfolding of *E. coli* SlyD* are reversible (51). Thermally induced unfolding can be monitored by near-UV CD spectroscopy. The CD signal originates from the tyrosine residues of the SlyD variants and shows a maximum of ~ 40 deg cm² dmol⁻¹ at 278 nm in the folded protein. It disappears when the tertiary structure collapses during the unfolding process (Figure 3A). All SlyD* variants exhibited similar near-UV CD spectra, pointing to a common nativelike conformation. Figure 3B shows the thermal unfolding transitions of the various truncated SlyD proteins as detected by CD at 278 nm. All of them unfold reversibly with different stabilities, and the T_M values range from 33.4 to 49.5 °C (Table 1). Near-UV CD spectra were recorded before and after the thermal unfolding–refolding cycles and were found to coincide.

The thermal unfolding transitions of the various SlyD* proteins as measured by near-UV CD are independent of the protein concentration between 25 and 250 μ M. A similar result was obtained when the difference in absorption at 288 nm was used as a probe. The UV-detected thermally induced unfolding transitions of 10 and 100 μ M SlyD also coincided, and the T_M values from the UV-detected unfolding transitions correspond well with those from the near-UV CD-detected melting curves (Table 1). This confirms the monomeric nature of the various SlyD* variants. GdmCl-induced unfold-

ing transitions were measured by near-UV CD as well. The stabilities of all SlyD* variants are very low. The transition midpoints were all below 1.0 M, and the GdmCl-induced transitions were also independent of protein concentration (data not shown).

SlyD* Exhibits High Folding Activity and Michaelis–Menten Kinetics. SlyD has been reported to catalyze prolyl isomerizations in both proteins and peptides (28, 33, 61). The catalytic efficiency of SlyD was fairly high with a protein substrate (40), but barely detectable when assayed with proline-containing peptides (33). This is reminiscent of the trigger factor, which, in protein folding reactions, combines a high prolyl isomerase activity with a chaperone function (40, 41, 47). Here, we investigated the efficiencies of the various C-terminally truncated SlyD molecules (SlyD*) in the catalysis of a proline-limited protein folding reaction. Reduced and carboxymethylated RNase T1 (RCM-T1) was used as the model substrate. Its refolding reaction is accompanied by a strong increase in tryptophan fluorescence and can be induced by increasing the NaCl concentration (48–50).

SlyD* from *E. coli* catalyzes the refolding of RCM-T1 very well. In the presence of ~ 2 nM SlyD*, refolding of RCM-T1 is already 2-fold accelerated (Figure 4A). The apparent first-order rate constant of folding k_{app} increases linearly with SlyD* concentration (Figure 4B). From the slope of this plot, a specificity constant k_{cat}/K_M of 0.68×10^6 M⁻¹ s⁻¹ was determined. Similarly, high catalytic efficiencies were found for almost all SlyD* homologues.

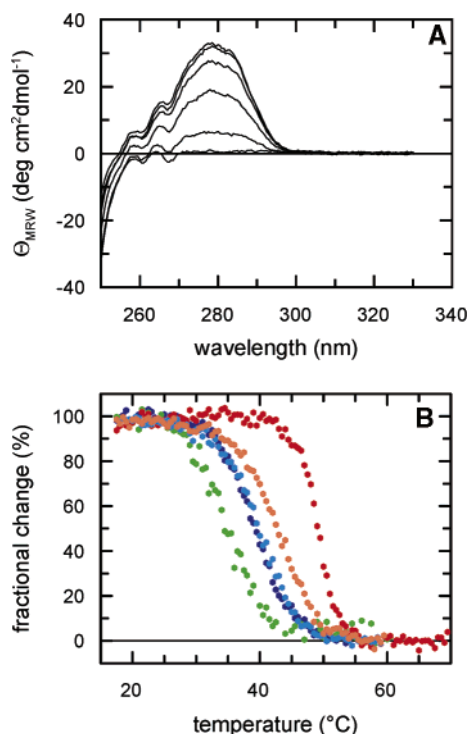


FIGURE 3: Unfolding of SlyD*. (A) CD spectra of 360 μM *E. coli* SlyD*(1–165) in the near-UV region in the presence of (from top to bottom) 0, 0.3, 0.6, 0.9, 1.2, and 1.5 M GdmCl in 50 mM sodium phosphate (pH 7.8), 100 mM sodium chloride, and 1 mM EDTA at 20 $^{\circ}\text{C}$. (B) Thermally induced unfolding transitions of SlyD* from *Y. pestis* (green), *T. pallidum* (dark blue), *V. cholerae* (light blue), *E. coli* (orange), and *P. multocida* (red). Unfolding was monitored by CD at 278 nm and normalized to the fractional change. Protein concentrations were 250 μM in 50 mM sodium phosphate (pH 7.8), 100 mM NaCl, and 1 mM EDTA.

Only the protein from *T. pallidum* was less active (Table 2). With values between $0.65 \times 10^6 \text{ M}^{-1} \text{ s}^{-1}$ (*Y. pestis*) and $1.2 \times 10^6 \text{ M}^{-1} \text{ s}^{-1}$ (*P. multocida*), most SlyD* homologues show catalytic efficiencies as high as that of the trigger factor (40, 41, 47). Except for *T. pallidum* SlyD* ($k_{\text{cat}}/K_{\text{M}} \sim 0.12 \times 10^6 \text{ M}^{-1} \text{ s}^{-1}$), the $k_{\text{cat}}/K_{\text{M}}$ values are ~ 100 -fold higher than the value determined for human FKBP12 ($k_{\text{cat}}/K_{\text{M}} = 0.014 \times 10^6 \text{ M}^{-1} \text{ s}^{-1}$) (41).

To find out why SlyD* is such an efficient folding enzyme, we measured the enzyme kinetics of SlyD*-catalyzed folding and determined the individual kinetic parameters K_{M} and k_{cat} from a Michaelis–Menten plot. In these experiments, the concentration of the folding substrate RCM-T1 was varied from 0.1 to 20 μM , at a constant SlyD* concentration of 20 nM. The uncatalyzed refolding of RCM-T1 proceeds with a half-time of 400 s and was accounted for in the analysis of the data accounts for the refolding. The experiments and the analysis were performed as described for trigger factor (41) and parvulin (62).

The initial rates of folding catalyzed by SlyD* show saturation behavior and are described well by the Michaelis–Menten equation. The results for *E. coli* SlyD and *P. multocida* SlyD are depicted in panels A and B of Figure 5, respectively. The K_{M} values are in the micromolar range and are summarized in Table 2. Four of the five SlyD* variants bind the refolding protein substrate with a K_{M} between ~ 0.34 and 1.65 μM ; only the affinity of SlyD* from *T. pallidum* is ~ 10 -fold weaker (17.3 μM). The turnover numbers are rather low, and range between 0.26 and 1.86 s^{-1} . The composite

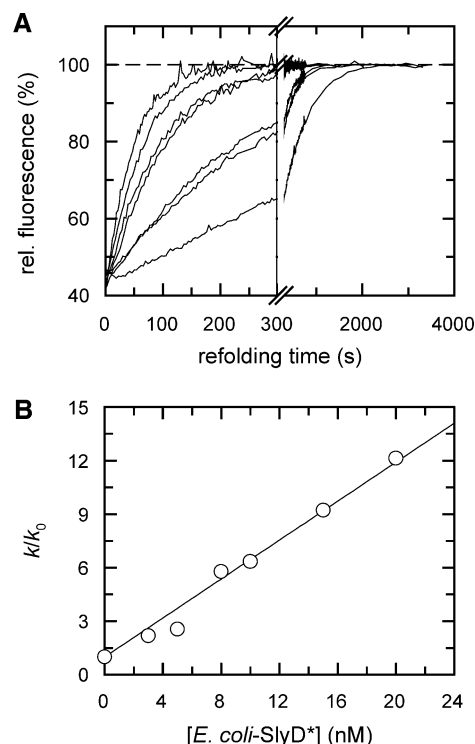


FIGURE 4: Refolding kinetics of RCM-T1 in the presence of increasing concentrations of *E. coli* SlyD* at 15 $^{\circ}\text{C}$. (A) The kinetics of refolding of 100 nM RCM-T1, as followed by the change in fluorescence at 320 nm, are shown in the presence of 0, 3, 5, 8, 10, 15, and 20 nM *E. coli* SlyD*. (B) Dependence on SlyD* concentration of the rate of slow folding. The ratio of the observed rate constants in the presence, k , and in the absence, k_0 , of SlyD* is shown as a function of the SlyD* concentration. A value of $0.68 \times 10^6 \text{ M}^{-1} \text{ s}^{-1}$ is obtained for $k_{\text{cat}}/K_{\text{M}}$ from the slope of the line in panel B. Refolding of RCM-T1 in 0.1 M Tris-HCl (pH 8.0) was initiated by dilution to 2.0 M NaCl in the same buffer.

value for the $k_{\text{cat}}/K_{\text{M}}$ ratios from this analysis agrees well with the above-described $k_{\text{cat}}/K_{\text{M}}$ estimates as obtained from Figure 4B, confirming that the enzyme kinetics of SlyD*-catalyzed folding are adequately described by the Michaelis–Menten model (Table 2).

The kinetic parameters for the C-terminally truncated SlyD variants almost coincide with the data for the full-length wild-type proteins. Wild-type SlyD from *E. coli*, for instance, displays a specificity constant of $0.59 \times 10^6 \text{ M}^{-1} \text{ s}^{-1}$, a value which compares well with the catalytic efficiency of $0.68 \times 10^6 \text{ M}^{-1} \text{ s}^{-1}$ for SlyD*. Since the *E. coli* SlyD* variants studied so far comprised the cysteine-free, presumably unstructured part of the C-terminal tail (residues 147–165), we designed a further truncated variant, SlyD**(1–148), which solely encompasses the N-terminal FKBP-like domain. This variant is also indistinguishable from SlyD*(1–165) and wild-type SlyD with respect to its specificity constant of $0.62 \times 10^6 \text{ M}^{-1} \text{ s}^{-1}$. This indicates that both prolyl isomerase and chaperone activity are localized in the N-terminal FKBP-like domain of SlyD. The C-terminal tail does not seem to support the binding of peptide or protein substrates to SlyD.

SlyD* Folding Activity Is Inhibited by Permanently Unfolded Proteins Irrespective of Their Proline Content. The high affinity of the SlyD variants for unfolded RCM-T1 suggests that other unfolded proteins might compete with the binding of RCM-T1 and inhibit the catalysis of folding.

Table 2: Enzyme Kinetic and Inhibition Parameters for Catalysis of RCM-T1 Folding by the SlyD Variants

prolyl isomerase	RCM-T1 refolding ^a	Michaelis–Menten experiments ^b			inhibition experiments ^c			
	specificity constant k_{cat}/K_M ($\text{M}^{-1} \text{s}^{-1}$)	turnover number k_{cat} (s^{-1})	Michaelis constant K_M (μM)	composite value k_{cat}/K_M ($\text{M}^{-1} \text{s}^{-1}$)	$K_{\text{i-app}}$ (RCM- α -La) (μM)	$K_{\text{i-app}}$ (RCM-Ten) (μM)	$K_{\text{i-app}}$ (RCM-T1-P39A) (μM)	$K_{\text{i-app}}$ (FK506) (μM)
<i>E. coli</i> SlyD(1–196)	0.59×10^6	nd ^d	nd ^d	nd ^d	1.5	0.22	0.19	4.6
<i>E. coli</i> SlyD*(1–165)	0.68×10^6	0.70	1.65	0.43×10^6	2.3	0.42	0.16	4.6
<i>E. coli</i> SlyD*(1–148)	0.62×10^6	nd ^d	nd ^d	nd ^d	1.7	0.07	0.14	4.3
<i>Y. pestis</i> SlyD*(1–165)	0.65×10^6	0.65	0.77	0.84×10^6	4.6	0.16	0.18	2.9
<i>V. cholerae</i> SlyD*(1–157)	1.10×10^6	0.26	0.34	0.76×10^6	2.3	1.3	0.07	1.2
<i>T. pallidum</i> SlyD*(1–160)	0.12×10^6	1.86	17.31	0.11×10^6	1.6	2.7	1.13	7.5
<i>P. multocida</i> SlyD*(1–156)	1.20×10^6	0.66	0.88	0.75×10^6	0.7	0.12	0.16	1.9

^a The k_{cat}/K_M values were obtained as described in the legend of Figure 4. ^b The kinetic experiments were performed as described in the legend of Figure 5. ^c The inhibition data were obtained from experiments as described in the legends of Figures 6 and 7. ^d Not determined.

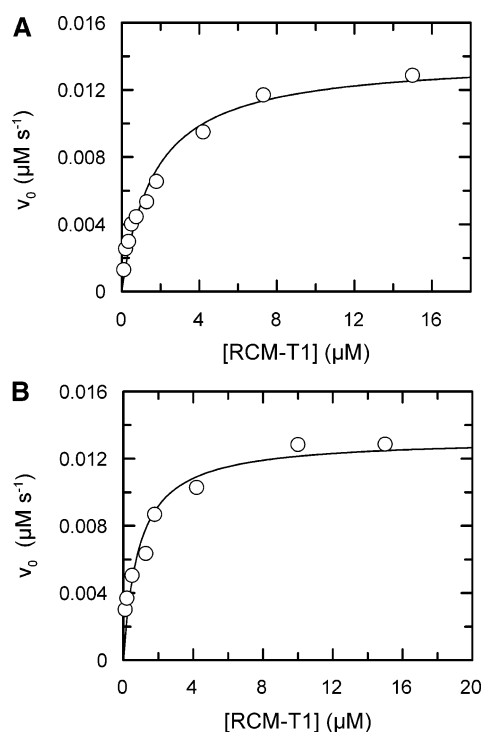


FIGURE 5: Michaelis–Menten kinetics of the refolding of RCM-T1 catalyzed by SlyD* from *E. coli* (A) and from *P. multocida* (B). The initial velocities of catalyzed refolding at 15 °C are shown as a function of the concentration of RCM-T1. The concentration of SlyD* was 20 nM, and the buffer consisted of 0.1 M Tris-HCl (pH 8.0) and 2.0 M NaCl. For *E. coli* SlyD*, values for K_M of 1.65×10^{-6} M and for k_{cat} of 0.7 s^{-1} were obtained from the analysis of the data. For *P. multocida* SlyD*, values for K_M of 0.88×10^{-6} M and for k_{cat} of 0.66 s^{-1} were obtained. The initial folding rates were determined and analyzed as described in Materials and Methods.

To investigate such an inhibition, we used the reduced and carboxymethylated form of α -lactalbumin (RCM- α -La) as a competitor. RCM- α -La adopts an extended conformation, and it remains soluble and unfolded when diluted into the refolding buffer of RCM-T1. RCM- α -La is thus a good substrate for chaperones (63) and a competitive inhibitor of the prolyl isomerase activities of trigger factor (41, 64) and of FkpA (65). RCM- α -La inhibits the prolyl isomerase activity of SlyD* with apparent inhibition constants in the micromolar range (Table 2). For *E. coli* SlyD*, a 30% inhibition is observed in the presence of $1.0 \mu\text{M}$ RCM- α -La.

A pronounced inhibition of the prolyl isomerase activity of SlyD* was observed even when the competing unfolded

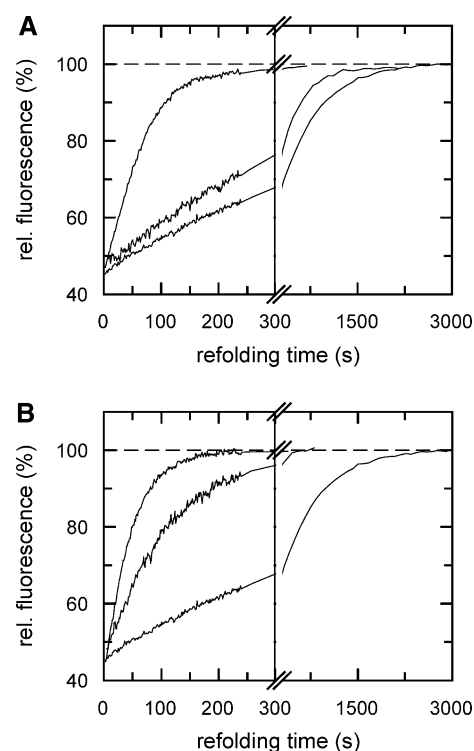


FIGURE 6: Inhibition of SlyD** [SlyD(1–148)]-catalyzed refolding of RCM-T1 by the unfolded polypeptide chains of (A) RCM-Ten-P7A/P9A/P50A and (B) RCM-T1-P39A. Shown is (from top to bottom) the refolding of RCM-T1 in the presence of SlyD**, and in the presence of SlyD** and inhibitory protein and the spontaneous folding of RCM-T1 in the absence of SlyD**. The concentration of SlyD** was 20 nM, and the concentration of the inhibitory proteins was $1.2 \mu\text{M}$ for RCM-Ten-P7A/P9A/P50A and $1.0 \mu\text{M}$ for RCM-T1-P39A. Otherwise, the refolding experiments were carried out as described in the legend of Figure 4 and in Materials and Methods.

protein lacked proline residues. The α -amylase inhibitor Tendamistat contains three proline residues, and its native form is stabilized by two disulfide bonds (66). As α -lactalbumin, it unfolds when these disulfide bonds are opened by reduction and subsequent carboxymethylation (67). In the P7A/P9A/P50A variant, all three proline residues are changed to alanine (68, 69). We find that unfolded Tendamistat molecules without the proline residues inhibit the catalyzed folding of RCM-T1 very well (Figure 6A).

The P39A variant of RNase T1 lacks the proline (Pro39), which determines the rate of slow folding of this protein, and its RCM form is permanently unfolded (70–72). This protein also inhibits the catalyzed refolding of RCM-T1 very

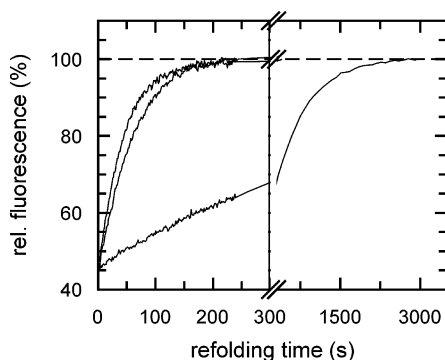


FIGURE 7: Inhibition of SlyD*-catalyzed refolding of RCM-T1 by FK506. The figure shows the proline-limited refolding of 100 nM RCM-T1 in the presence of 20 nM SlyD* with and without FK506 at its solubility limit of $\sim 2.0 \mu\text{M}$ (curves at the top). The uncatalyzed refolding of RCM-T1 is shown as a reference (bottom curve). To cope with the limited solubility of FK506 and to facilitate complex formation, SlyD and FK506 were preincubated at equimolar concentrations in a $2.0 \mu\text{M}$ stock solution. Then, the SlyD–FK506 complex was diluted into the thermostated refolding buffer at 15°C , which also contained $2.0 \mu\text{M}$ FK506. Subsequently, refolding was initiated by adding unfolded RCM-T1. In the reference experiment (uninhibited SlyD-catalyzed refolding of RCM-T1, top line), the small amount of ethanol originating from the 2.0 mM stock solution of FK506 in ethanol was accounted for.

efficiently (Figure 6B). Comparable results were obtained for the other SlyD* variants. The extent of inhibition by RCM-T1-P39A is similar in all cases, and the apparent inhibition constant is in the low micromolar range (Table 2). Together, these data suggest that the SlyD variants bind to unfolded proteins with rather high affinity. This affinity is independent of the presence of proline residues, and it forms the basis for the good binding to unfolded protein molecules and thus for the high folding activities of the SlyD variants. This is strongly reminiscent of trigger factor, which also recognizes and binds unfolded polypeptide substrates well, irrespective of their proline content (44, 45).

Refolding Activity of SlyD* Is Inhibited by FK506. SlyD is a FKBP-type prolyl isomerase (29, 38), and seven of 14 amino acids that are assumed to be important for FK506 binding by hFKBP12 (73) are conserved in SlyD (Figure 2); however, hitherto attempts to demonstrate inhibition by FK506 in peptide-based prolyl isomerase assays have been unsuccessful (28). If the affinity of SlyD for FK506 is low, it cannot be detected in the prolyl isomerase assay with the synthetic peptides of the Suc-Ala-Xaa-Pro-Phe-pNA type. The affinity for small peptide substrates is also low, and therefore, they must be used at a high concentration ($\sim 100 \mu\text{M}$) in the assays. Necessarily, the apparent affinity of SlyD for FK506 is further reduced in the presence of excess peptide substrate. Due to the poor solubility of FK506 in aqueous buffers [$< 2.0 \mu\text{M}$ in water at 25°C (74)], its effective concentration cannot be sufficiently increased to compete with the proline-containing peptides for binding to the active site of SlyD. In contrast, the affinity of SlyD* for RCM-T1 is high, and catalyzed folding can be followed with very high sensitivity at very low protein concentrations. The refolding assays were performed with 100 nM RCM-T1 and 20 nM SlyD*. Under these conditions, the SlyD*-catalyzed refolding of RCM-T1 is significantly decelerated in the presence of $\sim 2.0 \mu\text{M}$ FK506 (Figure 7). From the extent of inhibition, the fraction of SlyD* in complex with FK506 may

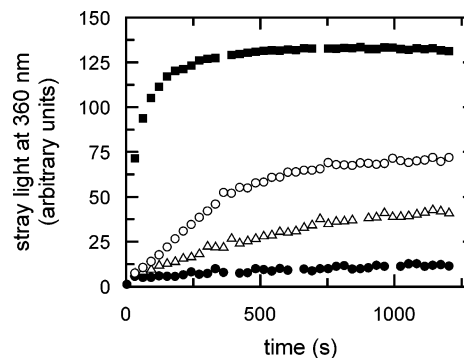


FIGURE 8: Influence of *E. coli* SlyD* single-chain variants on the aggregation of chemically denatured citrate synthase at 25°C . Denatured citrate synthase was diluted to a final concentration of $0.15 \mu\text{M}$ (monomer) in 50 mM Tris-HCl (pH 8.0), 60 mM GdmCl, 50 mM NaCl, and 0.2 mM DTE. Light scattering at 360 nm was monitored in the presence of $3.0 \mu\text{M}$ SlyD* [single SlyD (\circ)], in the presence of $1.5 \mu\text{M}$ SlyD*–SlyD* [tandem SlyD (Δ)], in the presence of $1.0 \mu\text{M}$ SlyD*–SlyD*–SlyD* [triple SlyD (\bullet)], and in the absence of chaperone (\blacksquare).

be determined, thus allowing a tentative calculation of the apparent inhibition constant. Indeed, the affinity of SlyD* for FK506 is rather low. The apparent dissociation constants range between 1.2 and $7.5 \mu\text{M}$ (Table 2), suggesting that FK506 binds to SlyD* ~ 3 orders of magnitude weaker than to human FKBP12 (73, 75–77). Interestingly, trigger factor from *E. coli* shows a similarly weak binding to FK506 with an apparent inhibition constant in the low micromolar range (B. Eckert and F. X. Schmid, unpublished observation). Both SlyD and trigger factor may thus be regarded as genuine but low-affinity FK506 binding proteins.

Single-Chain Variants of SlyD* Are Excellent Chaperones. With their high affinity for unfolded proteins, the SlyD* orthologues should also be active in chaperone assays. The assay developed by Buchner and co-workers exploits the strong aggregation tendency of folding intermediates of citrate synthase. When diluted with refolding buffer after thermally induced or denaturant-induced unfolding, citrate synthase aggregates spontaneously, which is accompanied by a strong increase in light scattering (57, 78). SlyD* from *E. coli* suppresses the aggregation of citrate synthase very efficiently when present in superstoichiometric amounts (Figure 8). Similar results were obtained with the SlyD* homologues from *Y. pestis*, *V. cholerae*, and *P. multocida*. SlyD* from *T. pallidum* suppressed the aggregation of citrate synthase less efficiently, in agreement with its lower affinity for unfolded RCM-T1. Human FKBP12 had no effect on the aggregation of citrate synthase (data not shown).

Recently, we found that the fusion of one or two SlyD* or FkpA modules strongly protected viral envelope proteins from aggregation (51). We therefore connected two or three SlyD* modules with each other via flexible, glycine-rich linkers and investigated their chaperone properties in the assay with citrate synthase. At equal concentrations of SlyD* subunits, the covalently linked dimers and trimers suppressed aggregation much better than the single SlyD* variant (Figure 8).

SlyD* Variants Are Well Suited to Being Fusion Modules. Fusions with truncated versions of SlyD or FkpA from *E. coli* are well suited to solubilizing aggregation-prone viral envelope proteins (51). After being expressed in *E. coli*, these fusion polypeptides could be easily purified and refolded,

yielding nativelike immunologically reactive forms of these target proteins. We now investigated whether the SlyD* homologues from the different species possess a similarly high chaperoning potential. As the target protein we chose a variant of the gp41 ectodomain fragment 536–681 [numbering from Chan et al. (79)] from HIV-1, which spontaneously and quantitatively aggregates in physiological buffer (51). In HIV-1-infected individuals, the gp41 ectodomain is the preferred target of the humoral immune response (80–82). Because of its pivotal role in membrane fusion, it is highly conserved among the nine HIV-1 subtypes, and peptide segments from the immunodominant loop region are well suited to serving immunodiagnostic purposes (81, 83, 84). Yet, its very strong tendency to aggregate renders the gp41 ectodomain a very difficult target for in vitro refolding, and simple and reliable renaturation protocols of recombinant gp41 are very much needed.

Two SlyD* modules from *Y. pestis* or from *T. pallidum* were fused in tandem to the amino terminus of gp41. These two SlyD* variants are 87 and 42% identical with SlyD* from *E. coli*, respectively, and represent the closest and the most distant homologue of this study (Figure 2). The chaperone modules were linked to the target protein via a flexible linker rich in glycine and serine residues, and hexahistidine tags were attached to the C-termini. Both fusion proteins were overproduced very efficiently in *E. coli* and accumulated as insoluble inclusion bodies in the host cytosol. The gp41 ectodomain alone is expressed very poorly in *E. coli*. After lysis with 7.0 M GdmCl and matrix-assisted refolding on a Ni–NTA column, the fusion proteins could be eluted in soluble form. Alternatively, the two fusion proteins could be refolded by renaturing gel filtration. To this end, the GdmCl-unfolded proteins were eluted in the presence of 7.0 M GdmCl from the Ni–NTA column by lowering the pH and applied on a Superdex 200 column which was pre-equilibrated with refolding buffer [50 mM sodium phosphate (pH 7.5), 100 mM NaCl, and 1 mM EDTA]. Like the fusion proteins of gp41 with SlyD* from *E. coli*, those with SlyD* from *T. pallidum* and from *Y. pestis* eluted as soluble oligomers with an apparently 3-fold symmetry (trimers, hexamers, and nonamers). These oligomeric states are determined by the target molecule gp41, which forms a trimeric coiled coil via an extended heptad repeat in its N-helical part (79, 85, 86). The nativelike fold of the SlyD*–SlyD*–gp41 fusion protein was verified under physiological conditions by near-UV CD spectroscopy as described previously (51). To test their immunological properties (i.e., their binding to anti-gp41 antibodies), *T. pallidum* SlyD*–SlyD*–gp41, *Y. pestis* SlyD*–SlyD*–gp41, and *E. coli* SlyD*–SlyD*–gp41 proteins were assessed with HIV-1 positive sera in an immunoassay as described in Materials and Methods. The measurements were carried out in the double-antigen sandwich format with different SlyD* modules on the capture and signaling side, respectively. All tested SlyD*–SlyD*–gp41 variants were highly reactive and clearly discriminated between HIV-1 positive and negative samples (Table 3). Subtypes B (United States and Europe), C (South Africa), and E (Asia) of the M group of HIV-1 are equally well recognized, ensuring the reliable diagnosis of the strongly diversifying lentiviral pathogen (87).

Two SlyD* modules in tandem are thus very efficient in solubilizing the target protein gp41. SlyD* from *T. pallidum* performed less well as a catalyst of RCM-T1 refolding and as a chaperone of citrate synthase, but in covalent fusion with the target protein, it was as efficient as the other SlyD* modules. Apparently, the covalent linkage to the target protein increased the effective concentration and thus enhanced the chaperone function of the SlyD* modules. When human FKBP12 was fused to the gp41 ectodomain fragment, the resulting fusion protein aggregated quantitatively after matrix-coupled refolding and imidazole elution (data not shown). Obviously, hFKBP12 is not able to confer solubility on an extremely hydrophobic target such as the gp41 ectodomain fragment. This is in line with its lack of chaperone activity in the citrate synthase assay and with the very poor catalysis of the refolding of RCM-T1.

DISCUSSION

SlyD is a folding helper with prolyl isomerase and chaperone properties. These functions reside in the N-terminal FKBP-like part of the molecule and are conserved within the SlyD family. The SlyD* orthologues from five different bacteria (*E. coli*, *Y. pestis*, *T. pallidum*, *V. cholerae*, and *P. multocida*) were all monomeric proteins with very high solubilities (>100 mg/mL). Both thermal and GdmCl-induced unfolding transitions were reversible, but the thermodynamic stabilities were low, with transition midpoints between 34 and 49 °C.

The refolding of RCM-T1 is limited in rate by the *trans*–*cis* isomerization of the peptidyl prolyl bond between Tyr38 and Pro39, and four of the five SlyD* homologues catalyzed this folding reaction very efficiently, with specificity constants (k_{cat}/K_M) of $\sim 1 \times 10^6 \text{ M}^{-1} \text{ s}^{-1}$ at 15 °C. This catalytic efficiency is extraordinarily high and exceeds the efficiency of the related hFKBP12 by a factor of ~ 100 . SlyD from *T. pallidum* was 5–10-fold less active than the other SlyD* homologues. The high specificity constants originate mainly from a tight binding to unfolded or refolding proteins ($K_M \sim 1 \mu\text{M}$). This high affinity for unfolded polypeptide chains is confirmed by two additional findings. First, all SlyD* proteins are inhibited in a seemingly competitive fashion by soluble and permanently unfolded protein chains, and second, the SlyD* homologues exhibit chaperone properties and suppress the aggregation of citrate synthase very efficiently. The unfolded protein chains do not need to contain proline residues to be recognized and bound by SlyD.

Such a combination of prolyl isomerase and chaperone activity is reminiscent of the trigger factor (40, 41, 47) and FkpA (65, 88). Both proteins contain FKBP-like domains and are thought to be involved in in vivo folding: trigger factor as a midwife at the ribosomal cradle of nascent chains (25–27, 47) and FkpA as an usher at the translocons of the periplasmic membrane (23). SurA, a parvulin-like prolyl isomerase in the *E. coli* periplasm (22, 89), also possesses chaperone features and is involved in the maturation of outer membrane proteins (90–92). The SlyD-like protein SlpA (28) is closely related to SlyD, but its function has not been characterized. In *E. coli*, thus at least four of its 10 prolyl isomerases are also active as chaperones, suggesting that efficient binding to unfolded or partially folded protein chains is important for the good performance of these prolyl

Table 3: Immunological Reactivity of gp41 Fusion Proteins Comprising SlyD* Variants from Different Species^a

HIV-1 negative sera	<i>T. pallidum</i> SlyD*–SlyD*–gp41–biotin (capture antigen) with <i>E. coli</i> SlyD*–SlyD*–gp41–ruthenium (signaling antigen)		<i>T. pallidum</i> SlyD*–SlyD*–gp41–biotin (capture antigen) with <i>Y. pestis</i> SlyD*–SlyD*–gp41–ruthenium (signaling antigen)	
	counts	relative signal	counts	relative signal
Salzburg 57	1558	1.23	5536	1.05
Salzburg 371	1154	0.91	4970	0.94
Salzburg 359	1171	0.93	4965	0.94
700–1101	1566	1.24	5907	1.12
700–1102	1237	0.98	5314	1.01
700–1103	1204	0.95	5314	1.01
700–1104	1183	0.94	5169	0.98
700–1105	1138	0.90	4886	0.93
700–1106	1193	0.95	5291	1.00
700–1107	1221	0.97	5408	1.03
average value of negative sera	1263	1.00	5276	1.00

HIV-1 positive sera	counts	relative signal	counts	relative signal
79–16 (HIV-1/E)	514 404	407.40	981 492	186.03
79–34 (HIV-1/E)	201 221	159.36	492 246	93.30
79–51 (HIV-1/E)	263 475	208.67	558 321	105.82
78–1 (HIV-1/B)	462 101	365.97	807 329	153.02
78–9 (HIV-1/B)	119 015	94.26	196 917	37.32
78–13 (HIV-1/B)	281 999	223.34	444 009	84.16
40–20 (HIV-1/C)	42 920	33.99	104 113	19.73
Milan 64 (HIV-1/B)	96 950	76.78	289 084	54.79
Milan 79 (HIV-1/B)	80 267	63.57	203 617	38.59

^a The immunoassays were performed in the double-antigen sandwich format by using an Elecsys 2010 analyzer as described in Materials and Methods. The antigen concentration was 750 ng/mL. The relative signals are normalized relative to the average value obtained for the HIV-1 negative samples. The HIV-1 positive sera were purchased from the Red Cross, Thailand, from NBTS Durban (Natal, South Africa), and from Milan Analytica AG (Milan, Switzerland); the HIV-1 negative controls were purchased from the Blutbank Salzburg (Salzburg, Austria).

isomerases. However, the physiological relevance of the prolyl isomerase activities of trigger factor and SurA and the relation to their chaperone function are still controversial (22, 93).

Folding helpers with both prolyl isomerase and chaperone activity are conserved in evolution. *Mycoplasma genitalium*, an organism with a very small genome, harbors the trigger factor as the only prolyl isomerase (94, 95). *Haemophilus influenzae*, another simple organism, contains only SlyD and trigger factor (96). The archaeon *Methanococcus thermolithotrophicus* contains only FKBP17, a putative SlyD homologue (97, 98).

Why is SlyD a much better chaperone than FKBP12, even though the two proteins are related and share the same fold? The FKBP12 fold comprises five antiparallel β -strands, which are arranged around a short α -helix and form the hydrophobic FK506 binding pocket (99, 100). FKBP12 and SlyD differ mainly in the first β -strand (which is lacking in SlyD) and in the apex (residues 88–92 in hFKBP12) of the so-called flap domain (29, 36). SlyD bears a 47-residue insert in this flap segment, which opposes the entrance to the hydrophobic pocket, and thus, it possibly controls the access to the enzyme active site (101). This so-called IF domain (insert in flap) has been structurally characterized in *Mt*-FKBP17, and it seems to be conserved in various archaeal FKBP17s with prolyl isomerase and chaperone features (98). On the basis of deletion experiments, it has been suggested that the flap insert constitutes the chaperone domain of *Mt*-FKBP17 (102). The flap insert of SlyD is 58% homologous with this region of *Mt*-FKBP17 (98) and possibly also forms part of the polypeptide binding site.

The cellular function and the physiological substrates of SlyD are essentially unknown. The bacteriophage ϕ X174 lysis protein E is an unphysiological substrate. This protein with 91 amino acids is involved in the inhibition of bacterial cell wall synthesis (103), and it was suggested that SlyD might be necessary for the isomerization of one or more of the five proline residues in lysis protein E. The Leu20–Pro21 bond was especially suggested to be a target for the prolyl isomerase activity of SlyD (104). Alternatively, SlyD might bind nonspecifically to hydrophobic regions of lysis protein E. Recently, it was suggested that SlyD is involved in the assembly of metal clusters (30).

Proteins with combined prolyl isomerase and chaperone functions, such as SlyD* or FkpA, are promising tools for recombinant protein production. The covalent attachment of SlyD* homologues to the N-terminus of the notoriously aggregation-prone ectodomains of retroviral proteins, such as HIV gp41, led to highly soluble fusion proteins which are easy to handle and exhibit high reactivity in immunological assays. Probably, the covalently linked SlyD* modules do act cooperatively in chaperoning the hydrophobic target molecules. This cooperative mechanism might be due to the increase in the effective concentration of the SlyD* polypeptide binding sites. It remains to be seen whether the efficiencies of other chaperones can also be improved by tandem fusions of several copies. Avidity phenomena are generally found with polyvalently binding macromolecules such as pentameric IgM (immunoglobulins from the M class).

Both SlyD* and FkpA seem to form dynamic complexes with the target molecules to which they are attached. This is reminiscent of the trigger factor, which establishes a rapid

and dynamic equilibrium with unfolded polypeptide substrates (46). Addition *in trans* of SlyD* or FkpA to a gp41 refolding assay does not prevent aggregation of the ectodomain fragment (51). Thus, the soluble complex between SlyD* and the target molecule seems to be intramolecular rather than intermolecular in nature.

In some cases, it may be desirable to conduct the *in vitro* refolding of SlyD*-X or FkpA-X fusion proteins as a sequential process. In a first step, the denaturant concentration would be adapted to allow refolding of the chaperone and to keep the target protein unfolded. In a second step, refolding of the target protein would be induced by further reducing the denaturant concentration. This technique requires that the chaperone module be significantly more stable than the target module. It seems therefore promising to search for SlyD or FkpA variants in thermophilic organisms. FKBP17 from *Methanococcus thermolithotrophicus* (98, 105) and FKBP18 from *Thermococcus* sp. KS-1 (106, 107) might be attractive candidates. TcFKBP18 improved the soluble expression of antibody fragments and of a putative rhodanese when used as a fusion module (108). However, a fusion protein comprising TcFKBP18 and the HIV-1 gp41 ectodomain fragment (536–681) aggregated rapidly (C. Scholz, unpublished observation), unlike the SlyD*-gp41 fusion protein, which is very soluble after matrix-coupled refolding (51).

Chaperones play an increasingly important role in the biotechnological production of soluble and functional proteins (109–112). Folding and purification of proteins are often facilitated by fusing them covalently with tags or partner proteins that fold robustly by themselves. The arsenal of fusion modules includes maltose binding protein (113), glutathione *S*-transferase (114), thioredoxin (115), NusA (116), DsbA (117, 118), and FkpA (51, 119). Their use customarily aims at improving the soluble expression (i.e., the native-like folding) of the respective target protein in either the cytosol or the periplasm of the overproducing *E. coli* host (120, 121). We suggest a strategy which exploits the excellent refolding properties of prolyl isomerases and chaperones such as SlyD and FkpA for *in vitro* renaturation of difficult target proteins. Fusions with SlyD* in particular promise to be very well suited to the functional solubilization of diagnostically or therapeutically important proteins.

ACKNOWLEDGMENT

We thank Dorothea Sizmann, Helmut Lenz, and Ralf Bollhagen (Roche Diagnostics GmbH) for helpful comments on the manuscript. We are indebted to Alfred Engel, Ariuna Bazarsuren, and Zhixin Shao (Roche Diagnostics GmbH) for cloning the TcFKBP18-gp41 expression cassette and for providing the wild-type SlyD overproducing BL21(DE3) strain. Thanks to Urban Schmitt for the Elecsys data, to Raimund Maier and Markus Zeeb (Universität Bayreuth) for help with the chaperone assays, to Hauke Lilie (Universität Halle-Wittenberg) for analytical ultracentrifugation data, and to Elke Faatz for supporting this publication. The excellent technical assistance of Franz Wagner, Friedrich Wiedemann, Laurence Thirault, Nicole Amtmann, Sima Hassanzadeh-Makooi, Achim Gärtner, and Markus Eckl (all Roche Diagnostics GmbH) is gratefully acknowledged. We thank H. Aygün, J. Engels, and T. Kiefhaber for a generous gift

of the proline-free variant of Tendamistat, and T. Schindler and L. M. Mayr for T1-P39A.

REFERENCES

- Kim, P. S., and Baldwin, R. L. (1990) Intermediates in the Folding Reactions of Small Proteins, *Annu. Rev. Biochem.* 59, 631–660.
- Jaenicke, R. (1987) Folding and Association of Proteins, *Prog. Biophys. Mol. Biol.* 49, 117–237.
- Jaenicke, R. (1992) Stability, Folding and Association of Proteins, *Fresenius' J. Anal. Chem.* 343, 9.
- Jaenicke, R. (1995) Folding and Association Versus Misfolding and Aggregation of Proteins, *Philos. Trans. R. Soc. London, Ser. B* 348, 97–105.
- Dobson, C. M. (2004) Principles of protein folding, misfolding and aggregation, *Semin. Cell Dev. Biol.* 15, 3–16.
- Jaenicke, R. (1993) What Does Protein Refolding *in vitro* Tell Us About Protein Folding in the Cell? *Philos. Trans. R. Soc. London, Ser. B* 339, 287–295.
- Schmid, F. X. (1991) Catalysis and assistance of protein folding, *Curr. Opin. Struct. Biol.* 1, 36–41.
- Ellis, R. J., and Hartl, F. U. (1999) Principles of protein folding in the cellular environment, *Curr. Opin. Struct. Biol.* 9, 102–110.
- Jaenicke, R. (1993) Role of Accessory Proteins in Protein Folding, *Curr. Opin. Struct. Biol.* 3, 104–112.
- Beissinger, M., and Buchner, J. (1998) How chaperones fold proteins, *Biol. Chem.* 379, 245–259.
- Buchner, J. (1996) Supervising the fold: Functional principles of molecular chaperones, *FASEB J.* 10, 10–19.
- Walter, S., and Buchner, J. (2002) Molecular chaperones: Cellular machines for protein folding, *Angew. Chem., Int. Ed.* 41, 1098–1113.
- Young, J. C., Agashe, V. R., Siegers, K., and Hartl, F. U. (2004) Pathways of chaperone-mediated protein folding in the cytosol, *Nat. Rev. Mol. Cell Biol.* 5, 781–791.
- Bukau, B., Deuerling, E., Pfund, C., and Craig, E. A. (2000) Getting newly synthesized proteins into shape, *Cell* 101, 119–122.
- Missiakas, D., and Raina, S. (1997) Protein folding in the bacterial periplasm, *J. Bacteriol.* 179, 2465–2471.
- Collet, J. F., and Bardwell, J. C. A. (2002) Oxidative protein folding in bacteria, *Mol. Microbiol.* 44, 1–8.
- Bardwell, J. C. A. (1994) Building Bridges: Disulfide Bond Formation in the Cell, *Mol. Microbiol.* 14, 199–205.
- Kadokura, H., Katzen, F., and Beckwith, J. (2003) Protein disulfide bond formation in prokaryotes, *Annu. Rev. Biochem.* 72, 111–135.
- Nakamoto, H., and Bardwell, J. C. A. (2004) Catalysis of disulfide bond formation and isomerization in the *Escherichia coli* periplasm, *Biochim. Biophys. Acta* 1694, 111–119.
- Bader, M. W., and Bardwell, J. C. A. (2002) Catalysis of disulfide bond formation and isomerization in *Escherichia coli*, *Adv. Protein Chem.* 59, 283–301.
- Rouvière, P. E., and Gross, C. A. (1996) SurA, a periplasmic protein with peptidyl-prolyl isomerase activity, participates in the assembly of outer membrane porins, *Gene Dev.* 10, 3170–3182.
- Behrens, S., Maier, R., de Cock, H., Schmid, F. X., and Gross, C. A. (2001) The SurA periplasmic PPIase lacking its parvulin domains functions *in vivo* and has chaperone activity, *EMBO J.* 20, 285–294.
- Arié, J. P., Sassoon, N., and Betton, J. M. (2001) Chaperone function of FkpA, a heat shock prolyl isomerase, in the periplasm of *Escherichia coli*, *Mol. Microbiol.* 39, 199–210.
- Bothmann, H., and Plückthun, A. (2000) The periplasmic *Escherichia coli* peptidyl-prolyl *cis/trans* isomerase FkpA. I. Increased functional expression of antibody fragments with and without *cis*-prolines, *J. Biol. Chem.* 275, 17100–17105.
- Deuerling, E., Schulze-Specking, A., Tomoyasu, T., Mogk, A., and Bukau, B. (1999) Trigger factor and DnaK cooperate in folding of newly synthesized proteins, *Nature* 400, 693–696.
- Ferbitz, L., Maier, T., Patzelt, H., Bukau, B., Deuerling, E., and Ban, N. (2004) Trigger factor in complex with the ribosome forms a molecular cradle for nascent proteins, *Nature* 431, 590–596.
- Hestekamp, T., Hauser, S., Lütcke, H., and Bukau, B. (1996) *Escherichia coli* trigger factor is a prolyl isomerase that associates with nascent polypeptide chains, *Proc. Natl. Acad. Sci. U.S.A.* 93, 4437–4441.

28. Hottenrott, S., Schumann, T., Plückthun, A., Fischer, G., and Rahfeld, J. U. (1997) The *Escherichia coli* SlyD is a metal ion-regulated peptidyl-prolyl *cis/trans*-isomerase, *J. Biol. Chem.* 272, 15697–15701.
29. Wülfing, C., Lombardero, J., and Plückthun, A. (1994) An *Escherichia coli* Protein Consisting of a Domain Homologous to FK506-Binding Proteins (FKBP) and a New Metal-Binding Motif, *J. Biol. Chem.* 269, 2895–2901.
30. Zhang, J. W., Butland, G., Greenblatt, J. F., Emili, A., and Zamble, D. B. (2005) A role for SlyD in the *Escherichia coli* hydrogenase biosynthetic pathway, *J. Biol. Chem.* 280, 4360–4366.
31. Porath, J. (1988) IMAC: Immobilized Metal-Ion Affinity Based Chromatography, *TrAC, Trends Anal. Chem.* 7, 254–259.
32. Arnold, F. H. (1991) Metal-Affinity Separations: A New Dimension in Protein Processing, *Bio/Technology* 9, 151–156.
33. Janowski, B., Wollner, S., Schutkowski, M., and Fischer, G. (1997) A protease-free assay for peptidyl-prolyl *cis/trans* isomerases using standard peptide substrates, *Anal. Biochem.* 252, 299–307.
34. Scholz, C., Maier, P., Dolinski, K., Heitman, J., and Schmid, F. X. (1999) R73A and H144Q mutants of the yeast mitochondrial cyclophilin Cpr3 exhibit a low prolyl isomerase activity in both peptide and protein folding assays, *FEBS Lett.* 443, 367–369.
35. Roof, W. D., and Young, R. (1995) ϕ -X174 Lysis Requires SlyD, a Host Gene Which Is Related to the FKBP Family of Peptidyl-Prolyl *Cis/Trans* Isomerases, *FEMS Microbiol. Rev.* 17, 213–218.
36. Roof, W. D., Fang, H. Q., Young, K. D., Sun, J. L., and Young, R. (1997) Mutational analysis of slyD, an *Escherichia coli* gene encoding a protein of the FKBP immunophilin family, *Mol. Microbiol.* 25, 1031–1046.
37. Bernhardt, T. G., Roof, W. D., and Young, R. (2002) The *Escherichia coli* FKBP-type PPIase SlyD is required for the stabilization of the E lysis protein of bacteriophage ϕ X174, *Mol. Microbiol.* 45, 99–108.
38. Roof, W. D., Horne, S. M., Young, K. D., and Young, R. (1994) SlyD, a Host Gene Required for ϕ -X174 Lysis, Is Related to the FK506-Binding Protein Family of Peptidyl-Prolyl *Cis/Trans*-Isomerases, *J. Biol. Chem.* 269, 2902–2910.
39. Hesterkamp, T., and Bukau, B. (1996) The *Escherichia coli* trigger factor, *FEBS Lett.* 389, 32–34.
40. Zarnt, T., Tradler, T., Stoller, G., Scholz, C., Schmid, F. X., and Fischer, G. (1997) Modular structure of the trigger factor required for high activity in protein folding, *J. Mol. Biol.* 271, 827–837.
41. Scholz, C., Stoller, G., Zarnt, T., Fischer, G., and Schmid, F. X. (1997) Cooperation of enzymatic and chaperone functions of trigger factor in the catalysis of protein folding, *EMBO J.* 16, 54–58.
42. Webb, H. M., Ruddock, L. W., Marchant, R. J., Jonas, K., and Klappa, P. (2001) Interaction of the periplasmic peptidyl-prolyl *cis/trans* isomerase SurA with model peptides: The N-terminal region of SurA is essential and sufficient for peptide binding, *J. Biol. Chem.* 276, 45622–45627.
43. Frech, C., Wunderlich, M., Glockshuber, R., and Schmid, F. X. (1996) Preferential binding of an unfolded protein to DsbA, *EMBO J.* 15, 392–398.
44. Patzelt, H., Rüdiger, S., Brehmer, D., Kramer, G., Vorderwülbecke, S., Schaffitzel, E., Waitz, A., Hesterkamp, T., Dong, L., Schneider-Mergener, J., Bukau, B., and Deuerling, E. (2001) Binding specificity of *Escherichia coli* trigger factor, *Proc. Natl. Acad. Sci. U.S.A.* 98, 14244–14249.
45. Scholz, C., Mücke, M., Rape, M., Pecht, A., Pahl, A., Bang, H., and Schmid, F. X. (1998) Recognition of protein substrates by the prolyl isomerase trigger factor is independent of proline residues, *J. Mol. Biol.* 277, 723–732.
46. Maier, R., Scholz, C., and Schmid, F. X. (2001) Dynamic association of trigger factor with protein substrates, *J. Mol. Biol.* 314, 1181–1190.
47. Stoller, G., Rücknagel, K. P., Nierhaus, K. H., Schmid, F. X., Fischer, G., and Rahfeld, J. U. (1995) A Ribosome-Associated Peptidyl-Prolyl *Cis/Trans* Isomerase Identified as the Trigger Factor, *EMBO J.* 14, 4939–4948.
48. Schmid, F. X., Frech, C., Scholz, C., and Walter, S. (1996) Catalyzed and assisted protein folding of ribonuclease T1, *Biol. Chem.* 377, 417–424.
49. Mayr, L. M., Odeley, C., Schutkowski, M., and Schmid, F. X. (1996) Kinetic analysis of the unfolding and refolding of ribonuclease T1 by a stopped-flow double-mixing technique, *Biochemistry* 35, 5550–5561.
50. Mücke, M., and Schmid, F. X. (1994) Folding Mechanism of Ribonuclease T1 in the Absence of the Disulfide Bonds, *Biochemistry* 33, 14608–14619.
51. Scholz, C., Schaarschmidt, P., Engel, A. M., Andres, H., Schmitt, U., Faatz, E., Balbach, J., and Schmid, F. X. (2005) Functional solubilization of aggregation-prone HIV envelope proteins by covalent fusion with chaperone modules, *J. Mol. Biol.* 345, 1229–1241.
52. Mücke, M., and Schmid, F. X. (1994) Intact Disulfide Bonds Decelerate the Folding of Ribonuclease T1, *J. Mol. Biol.* 239, 713–725.
53. Hochuli, E., Döbeli, H., and Schacher, A. (1987) New Metal Chelate Adsorbent Selective for Proteins and Peptides Containing Neighboring Histidine-Residues, *J. Chromatogr.* 411, 177–184.
54. Schagger, H., and von Jagow, G. (1987) Tricine Sodium Dodecyl-Sulfate Polyacrylamide-Gel Electrophoresis for the Separation of Proteins in the Range from 1 kDa to 100 kDa, *Anal. Biochem.* 166, 368–379.
55. Gill, S. C., and von Hippel, P. H. (1989) Calculation of protein extinction coefficients from amino acid sequence data, *Anal. Biochem.* 182, 319–326.
56. Pace, C. N., Vajdos, F., Fee, L., Grimsley, G., and Gray, T. (1995) How to Measure and Predict the Molar Absorption Coefficient of a Protein, *Protein Sci.* 4, 2411–2423.
57. Buchner, J., Grallert, H., and Jakob, U. (1998) Analysis of chaperone function using citrate synthase as nonnative substrate protein, *Methods Enzymol.* 290, 323–338.
58. Kofron, J. L., Kuzmic, P., Kishore, V., Colonbonilla, E., and Rich, D. H. (1991) Determination of Kinetic Constants for Peptidyl-Prolyl *Cis/Trans* Isomerases by an Improved Spectrophotometric Assay, *Biochemistry* 30, 6127–6134.
59. Mukherjee, S., Shukla, A., and Gupta, P. (2003) Single-step purification of a protein-folding catalyst, the SlyD peptidyl prolyl isomerase (PPI), from cytoplasmic extracts of *Escherichia coli*, *Biotechnol. Appl. Biochem.* 37, 183–186.
60. Mitterauer, T., Nanoff, C., Ahorn, H., Freissmuth, M., and Hohenegger, M. (1999) Metal-dependent nucleotide binding to the *Escherichia coli* rotamase SlyD, *Biochem. J.* 342, 33–39.
61. Satumba, W. J., and Mossing, M. C. (2002) Folding and assembly of λ cro repressor dimers are kinetically limited by proline isomerization, *Biochemistry* 41, 14216–14224.
62. Scholz, C., Rahfeld, J., Fischer, G., and Schmid, F. X. (1997) Catalysis of protein folding by parvulin, *J. Mol. Biol.* 273, 752–762.
63. Hayer-Hartl, M. K., Ewbank, J. J., Creighton, T. E., and Hartl, F. U. (1994) Conformational Specificity of the Chaperonin GroEL for the Compact Folding Intermediates of α -Lactalbumin, *EMBO J.* 13, 3192–3202.
64. Huang, G. C., Li, Z. Y., and Zhou, J. M. (2000) Conformational specificity of trigger factor for the folding intermediates of α -lactalbumin, *Biochim. Biophys. Acta* 1480, 77–82.
65. Ramm, K., and Plückthun, A. (2001) High enzymatic activity and chaperone function are mechanistically related features of the dimeric *E. coli* peptidyl-prolyl isomerase FkpA, *J. Mol. Biol.* 310, 485–498.
66. Vertesy, L., Oeding, V., Bender, R., Zepf, K., and Nesemann, G. (1984) Tendamistat (HOE 467), a tight-binding α -amylase inhibitor from *Streptomyces tendae* 4158. Isolation, biochemical properties, *Eur. J. Biochem.* 141, 505–512.
67. Vogl, T., Brengelmann, R., Hinz, H. J., Scharf, M., Lotzbeyer, M., and Engels, J. W. (1995) Mechanism of Protein Stabilization by Disulfide Bridges: Calorimetric Unfolding Studies on Disulfide-Deficient Mutants of the α -Amylase Inhibitor Tendamistat, *J. Mol. Biol.* 254, 481–496.
68. Pappenberger, G., Aygün, H., Engels, J. W., Reimer, U., Fischer, G., and Kiefhaber, T. (2001) Nonprolyl *cis* peptide bonds in unfolded proteins cause complex folding kinetics, *Nat. Struct. Biol.* 8, 452–458.
69. Pappenberger, G., Bachmann, A., Müller, R., Aygün, H., Engels, J. W., and Kiefhaber, T. (2003) Kinetic mechanism and catalysis of a native-state prolyl isomerization reaction, *J. Mol. Biol.* 326, 235–246.
70. Mayr, L. M., and Schmid, F. X. (1993) Kinetic Models for Unfolding and Refolding of Ribonuclease T1 with Substitution of *cis*-Proline-39 by Alanine, *J. Mol. Biol.* 231, 913–926.
71. Mayr, L. M., and Schmid, F. X. (1993) A Purification Method for Labile Variants of Ribonuclease T1, *Protein Expression Purif.* 4, 52–58.

72. Mayr, L. M., Landt, O., Hahn, U., and Schmid, F. X. (1993) Stability and Folding Kinetics of Ribonuclease T1 Are Strongly Altered by the Replacement of *cis*-Proline-39 with Alanine, *J. Mol. Biol.* 231, 897–912.
73. Kay, J. E. (1996) Structure–function relationships in the FK506-binding protein (FKBP) family of peptidyl-prolyl *cis/trans* isomerases, *Biochem. J.* 314, 361–385.
74. Arima, H., Yunomae, K., Miyake, K., Irie, T., Hirayama, F., and Uekama, K. (2001) Comparative studies of the enhancing effects of cyclodextrins on the solubility and oral bioavailability of tacrolimus in rats, *J. Pharm. Sci.* 90, 690–701.
75. Galat, A. (1993) Peptidylproline *Cis/Trans*-Isomerases: Immunophilins, *Eur. J. Biochem.* 216, 689–707.
76. Bierer, B. E., Mattila, P. S., Standaert, R. F., Herzenberg, L. A., Burakoff, S. J., Crabtree, G., and Schreiber, S. L. (1990) Two Distinct Signal Transmission Pathways in T Lymphocytes are Inhibited by Complexes Formed between an Immunophilin and either FK506 or Rapamycin, *Proc. Natl. Acad. Sci. U.S.A.* 87, 9231–9235.
77. Park, S. T., Aldape, R. A., Futer, O., Decenzo, M. T., and Livingston, D. J. (1992) PPIase Catalysis by Human Fk506-Binding Protein Proceeds through a Conformational Twist Mechanism, *J. Biol. Chem.* 267, 3316–3324.
78. Buchner, J., Schmidt, M., Fuchs, M., Jaenicke, R., Rudolph, R., Schmid, F. X., and Kiefhaber, T. (1991) GroEL Facilitates Refolding of Citrate Synthase by Suppressing Aggregation, *Biochemistry* 30, 1586–1591.
79. Chan, D. C., Fass, D., Berger, J. M., and Kim, P. S. (1997) Core structure of gp41 from the HIV envelope glycoprotein, *Cell* 89, 263–273.
80. Norrby, E., Biberfeld, G., Chiodi, F., Vongegerfeldt, A., Naucler, A., Parks, E., and Lerner, R. (1987) Discrimination between Antibodies to HIV and to Related Retroviruses Using Site-Directed Serology, *Nature* 329, 248–250.
81. Gnann, J. W., McCormick, J. B., Mitchell, S., Nelson, J. A., and Oldstone, M. B. A. (1987) Synthetic Peptide Immunoassay Distinguishes HIV Type-1 and HIV Type-2 Infections, *Science* 237, 1346–1349.
82. Gnann, J. W., Nelson, J. A., and Oldstone, M. B. A. (1987) Fine Mapping of an Immunogenic Domain in the Transmembrane Glycoprotein of the Human Immunodeficiency Virus, *Clin. Res.* 35, A614–A614.
83. Gnann, J. W., Schwimbeck, P. L., Nelson, J. A., Truax, A. B., and Oldstone, M. B. A. (1987) Diagnosis of AIDS by Using a 12-Amino Acid Peptide Representing an Immunodominant Epitope of the Human Immunodeficiency Virus, *J. Infect. Dis.* 156, 261–267.
84. Wang, J. J. G., Steel, S., Wisniewolski, R., and Wang, C. Y. (1986) Detection of Antibodies to Human T-Lymphotropic Virus Type III by Using a Synthetic Peptide of 21 Amino Acid Residues Corresponding to a Highly Antigenic Segment of gp41 Envelope Protein, *Proc. Natl. Acad. Sci. U.S.A.* 83, 6159–6163.
85. Gallaher, W. R. (1996) Similar structural models of the transmembrane proteins of Ebola and avian sarcoma viruses, *Cell* 85, 477–478.
86. Weissenhorn, W., Wharton, S. A., Calder, L. J., Earl, P. L., Moss, B., Aliprandis, E., Skehel, J. J., and Wiley, D. C. (1996) The ectodomain of HIV-1 env subunit gp41 forms a soluble, α -helical, rod-like oligomer in the absence of gp120 and the N-terminal fusion peptide, *EMBO J.* 15, 1507–1514.
87. Malim, M. H., and Emerman, M. (2001) HIV-1 sequence variation: Drift, shift, and attenuation, *Cell* 104, 469–472.
88. Ramm, K., and Plückthun, A. (2000) The periplasmic *Escherichia coli* peptidyl-prolyl *cis/trans*-isomerase FkpA. II. Isomerase-independent chaperone activity *in vitro*, *J. Biol. Chem.* 275, 17106–17113.
89. Missiakas, D., Betton, J. M., and Raina, S. (1996) New components of protein folding in extracytoplasmic compartments of *Escherichia coli* SurA, FkpA and Skp/OmpH, *Mol. Microbiol.* 21, 871–884.
90. Bitto, E., and McKay, D. B. (2003) The periplasmic molecular chaperone protein SurA binds a peptide motif that is characteristic of integral outer membrane proteins, *J. Biol. Chem.* 278, 49316–49322.
91. Hennecke, G., Nolte, J., Volkmer-Engert, R., Schneider-Mergener, J., and Behrens, S. (2005) The periplasmic chaperone SurA exploits two features characteristic of integral outer membrane proteins for selective substrate recognition, *J. Biol. Chem.* 280, 23540–23548.
92. Lazar, S. W., and Kolter, R. (1996) SurA assists the folding of *Escherichia coli* outer membrane proteins, *J. Bacteriol.* 178, 1770–1773.
93. Kramer, G., Patzelt, H., Rauch, T., Kurz, T. A., Vorderwülbecke, S., Bukau, B., and Deuerling, E. (2004) Trigger factor peptidyl-prolyl *cis/trans* isomerase activity is not essential for the folding of cytosolic proteins in *Escherichia coli*, *J. Biol. Chem.* 279, 14165–14170.
94. Fraser, C. M., Gocayne, J. D., White, O., Adams, M. D., Clayton, R. A., Fleischmann, R. D., Bult, C. J., Kerlavage, A. R., Sutton, G., Kelley, J. M., Fritchman, J. L., Weidman, J. F., Small, K. V., Sandusky, M., Fuhrmann, J., Nguyen, D., Utterback, T. R., Saudek, D. M., Phillips, C. A., Merrick, J. M., Tomb, J. F., Dougherty, B. A., Bott, K. F., Hu, P. C., Lucier, T. S., Peterson, S. N., Smith, H. O., Hutchison, C. A., and Venter, J. C. (1995) The Minimal Gene Complement of *Mycoplasma Genitalium*, *Science* 270, 397–403.
95. Bang, N., Pecht, A., Raddatz, G., Scior, T., Solbach, W., Brune, K., and Pahl, A. (2000) Prolyl isomerases in a minimal cell: Catalysis of protein folding by trigger factor from *Mycoplasma genitalium*, *Eur. J. Biochem.* 267, 3270–3280.
96. Fleischmann, R. D., Adams, M. D., White, O., Clayton, R. A., Kirkness, E. F., Kerlavage, A. R., Bult, C. J., Tomb, J. F., Dougherty, B. A., Merrick, J. M., McKenney, K., Sutton, G., Fitzhugh, W., Fields, C., Gocayne, J. D., Scott, J., Shirley, R., Liu, L. I., Glodek, A., Kelley, J. M., Weidman, J. F., Phillips, C. A., Spriggs, T., Hedblom, E., Cotton, M. D., Utterback, T. R., Hanna, M. C., Nguyen, D. T., Saudek, D. M., Brandon, R. C., Fine, L. D., Fritchman, J. L., Fuhrmann, J. L., Geoghegan, N. S. M., Gnehm, C. L., McDonald, L. A., Small, K. V., Fraser, C. M., Smith, H. O., and Venter, J. C. (1995) Whole-Genome Random Sequencing and Assembly of *Haemophilus Influenzae* Rd, *Science* 269, 496–512.
97. Furutani, M., Iida, T., Yamano, S., Kamino, K., and Maruyama, T. (1998) Biochemical and genetic characterization of an FK506-sensitive peptidyl-prolyl *cis/trans* isomerase from a thermophilic archaeon, *Methanococcus thermolithotrophicus*, *J. Bacteriol.* 180, 388–394.
98. Suzuki, R., Nagata, K., Yumoto, F., Kawakami, M., Nemoto, N., Furutani, M., Adachi, K., Maruyama, T., and Tanokura, M. (2003) Three-dimensional solution structure of an archaeal FKBP with a dual function of peptidyl-prolyl *cis/trans* isomerase and chaperone-like activities, *J. Mol. Biol.* 328, 1149–1160.
99. van Duyn, G. D., Standaert, R. F., Karplus, P. A., Schreiber, S. L., and Clardy, J. (1991) Atomic Structure of FKBP-FK506, an Immunophilin-Immunosuppressant Complex, *Science* 252, 839–842.
100. Michnick, S. W., Rosen, M. K., Wandless, T. J., Karplus, M., and Schreiber, S. L. (1991) Solution Structure of FKBP, a Rotamase Enzyme and Receptor for FK506 and Rapamycin, *Science* 252, 836–839.
101. Callebaut, I., and Mornon, J. P. (1995) Trigger Factor, One of the *Escherichia coli* Chaperone Proteins, Is an Original Member of the FKBP Family, *FEBS Lett.* 374, 211–215.
102. Furutani, M., Ideno, A., Iida, T., and Maruyama, T. (2000) FK506 binding protein from a thermophilic archaeon, *Methanococcus thermolithotrophicus*, has chaperone-like activity *in vitro*, *Biochemistry* 39, 453–462.
103. Bernhardt, T. G., Roof, W. D., and Young, R. (2000) Genetic evidence that the bacteriophage ϕ X174 lysis protein inhibits cell wall synthesis, *Proc. Natl. Acad. Sci. U.S.A.* 97, 4297–4302.
104. Witte, A., Schrot, G., Schön, P., and Lubitz, W. (1997) Proline 21, a residue within the α -helical domain of ϕ X174 lysis protein E, is required for its function in *Escherichia coli*, *Mol. Microbiol.* 26, 337–346.
105. Murayama, K., Shindo, N., Suzuki, R., Kawakami, M., Mineki, R., Taka, H., Kazuno, S., Nagata, K., Maruyama, T., and Tanokura, M. (2000) Characterization of native and recombinant peptidyl prolyl *cis/trans* isomerases derived from *Methanococcus thermolithotrophicus* based on cDNA sequence, *Electrophoresis* 21, 1733–1739.
106. Iida, T., Furutani, M., Nishida, F., and Maruyama, T. (1998) FKBP-type peptidyl-prolyl *cis-trans* isomerase from a sulfur-dependent hyperthermophilic archaeon, *Thermococcus* sp. KS-1, *Gene* 222, 249–255.
107. Ideno, A., Yoshida, T., Iida, T., Furutani, M., and Maruyama, T. (2001) FK506-binding protein of the hyperthermophilic archaeum, *Thermococcus* sp KS-1, a cold-shock-inducible peptidyl-prolyl *cis-*

- trans* isomerase with activities to trap and refold denatured proteins, *Biochem. J.* 357, 465–471.
108. Ideno, A., Furutani, M., Iwabuchi, T., Iida, T., Iba, Y., Kurosawa, Y., Sakuraba, H., Ohshima, T., Kwarabayashi, Y., and Maruyama, T. (2004) Expression of foreign proteins in *Escherichia coli* by fusing with an archaeal FK506 binding protein, *Appl. Microbiol. Biotechnol.* 64, 99–105.
109. Mogk, A., Mayer, M. P., and Deuerling, E. (2002) Mechanisms of protein folding: Molecular chaperones and their application in biotechnology, *ChemBioChem* 3, 807–814.
110. Wang, Q. H., Buckle, A. M., Foster, N. W., Johnson, C. M., and Fersht, A. R. (1999) Design of highly stable functional GroEL minichaperones, *Protein Sci.* 8, 2186–2193.
111. Altamirano, M. M., Garcia, C., Possani, L. D., and Fersht, A. R. (1999) Oxidative refolding chromatography: Folding of the scorpion toxin Cn5, *Nat. Biotechnol.* 17, 187–191.
112. Ehrnsperger, M., Hergersberg, C., Wienhues, U., Nichtl, A., and Buchner, J. (1998) Stabilization of proteins and peptides in diagnostic immunological assays by the molecular chaperone Hsp25, *Anal. Biochem.* 259, 218–225.
113. Diguan, C., Li, P., Riggs, P. D., and Inouye, H. (1988) Vectors That Facilitate the Expression and Purification of Foreign Peptides in *Escherichia coli* by Fusion to Maltose Binding Protein, *Gene* 67, 21–30.
114. Smith, D. B., and Johnson, K. S. (1988) Single-Step Purification of Polypeptides Expressed in *Escherichia coli* as Fusions with Glutathione S-Transferase, *Gene* 67, 31–40.
115. Wilkinson, D. L., Ma, N. T., Haught, C., and Harrison, R. G. (1995) Purification by Immobilized Metal Affinity-Chromatography of Human Atrial-Natriuretic-Peptide Expressed in a Novel Thioredoxin Fusion Protein, *Biotechnol. Prog.* 11, 265–269.
116. Davis, G. D., Elisei, C., Newham, D. M., and Harrison, R. G. (1999) New fusion protein systems designed to give soluble expression in *Escherichia coli*, *Biotechnol. Bioeng.* 65, 382–388.
117. Zhang, Y., Olsen, D. R., Nguyen, K. B., Olson, P. S., Rhodes, E. T., and Mascarenhas, D. (1998) Expression of eukaryotic proteins in soluble form in *Escherichia coli*, *Protein Expression Purif.* 12, 159–165.
118. Winter, J., Neubauer, P., Glockshuber, R., and Rudolph, R. (2000) Increased production of human proinsulin in the periplasmic space of *Escherichia coli* by fusion to DsbA, *J. Biotechnol.* 84, 175–185.
119. Zhang, Z., Song, L. P., Fang, M., Wang, F., He, D., Zhao, R., Liu, J., Zhou, Z. Y., Yin, C. C., Lin, Q., and Huang, H. L. (2003) Production of soluble and functional engineered antibodies in *Escherichia coli* improved by FkpA, *BioTechniques* 35, 1032–1042.
120. Terpe, K. (2003) Overview of tag protein fusions: From molecular and biochemical fundamentals to commercial systems, *Appl. Microbiol. Biotechnol.* 60, 523–533.
121. Mergulhao, F. J. M., Summers, D. K., and Monteiro, G. A. (2005) Recombinant protein secretion in *Escherichia coli*, *Biotechnol. Adv.* 23, 177–202.
122. Thompson, J. D., Higgins, D. G., and Gibson, T. J. (1994) *Clustal W*: Improving the Sensitivity of Progressive Multiple Sequence Alignment through Sequence Weighting, Position-Specific Gap Penalties and Weight Matrix Choice, *Nucleic Acids Res.* 22, 4673–4680.
123. Chenna, R., Sugawara, H., Koike, T., Lopez, R., Gibson, T. J., Higgins, D. G., and Thompson, J. D. (2003) Multiple sequence alignment with the Clustal series of programs, *Nucleic Acids Res.* 31, 3497–3500.

BI051922N